

Chapter 5 Global Phase Diagram for Binary Mixtures of “Hard Sphere + van der Waals” Molecules: Calculation with the Guggenheim Equation of State.

The fluid phase behaviour of binary mixtures has been comprehensively studied (Schneider, 1978, 1991; Brunner, 1988, 1990) over a wide range of both pressure and temperature. As discussed in Chapter 4, classification schemes (van Konynenburg and Scott, 1980; Nezbeda et al. 1997; Yelash and Kraska, 1998) have been developed based on the critical equilibria behaviour of binary mixtures and increasingly accurate equations of state (Chapter 3) have been reported and applied successfully to the prediction of binary mixture phenomena (van Pelt et al., 1991). The application of molecular simulation (Sadus, 1999a) to phase equilibria is expanding continually. Progress has also been reported recently for a classification scheme for ternary mixtures (Wei and Sadus, 1999a; Wei, 1998).

It is well documented (Sadus, 1992) that the phase behaviour of the majority of commonly occurring binary mixtures can be broadly classified by their critical properties in terms of one of six basic types (van Konynenburg and Scott, 1980). In Chapter 3, we reviewed the phase behaviour of binary mixtures. The phase behaviour of Types I to V mixtures can be predicted qualitatively using the simple van der Waals equation of state in which intermolecular interaction is modelled by combining a hard-sphere term for repulsion with a dispersion term. The van der Waals equation does not predict Type VI phenomena, which is characterized by both lower (LCST) and upper (UCST) critical phenomena resulting in closed-loop liquid-liquid immiscibility. For quantitative predictions, the van der Waals equation has been superseded by many more

accurate equations of state (Wei and Sadus, 2000). Type VI behaviour and closed-loop liquid-liquid equilibria are associated typically with aqueous mixtures (Sadus, 1992; Schneider, 1978). Type VI behaviour is predicted (Boshkov, 1987, refer Sadus, 1992) by a Lennard-Jones equation of state and more sophisticated approaches typified by equations of state that incorporate either temperature-dependent attractive terms (Boshkov and Yelash, 1998) or explicit contributions for hydrogen bonding (van Pelt et al., 1991).

It has been demonstrated recently (Yelash and Kraska, 1998) that Type VI phenomena can also be calculated using the Carnahan-Starling van der Waals (Carnahan and Starling, 1969) (CSvdW) equation of state. In this chapter, we investigate whether the Guggenheim equation of state can also predict the phase behaviour of all types of mixtures. Both the CSvdW and Guggenheim equations of state model the intermolecular interactions of fluids by combining an accurate hard-sphere repulsion term with simple van der Waals dispersion interactions in the spirit of the original van der Waals equation of state, but the Guggenheim equation has a considerably simpler hard-sphere term.

5.1 The Global Phase Diagram of Binary Mixtures for Equal Sized Molecules

We have determined the global phase diagram (Figure 5.1) of binary mixtures of hard-spheres of equal size by calculating the critical properties obtained from the Guggenheim equation of state. The calculation of critical equilibria and the thermodynamic criteria for the boundary states of the global phase diagram were given in Chapter 4.

We examined mixtures of components of equal size in the work. This eliminates size effects on the global phase diagram. The equivalence of size means that the components of the binary mixture are distinguished solely by differences in the f conformal or equivalently by differences in their critical temperatures (see Chapter 2). The nomenclature used here follows closely previous work (Yelash and Kraska, 1998) as given in Chapter 4 except that we illustrate the global phase diagram (Figure 5.1) by plotting the strength of unlike interaction (?) as a function of the logarithm of the ratio of the critical temperatures ($\log(T_{22}^C/T_{11}^C)$). We have adopted this approach because it provides a closer link with a real experimental quantity (the critical temperatures) than alternative approaches.

The overall global phase diagram (Figure 5.1) has the same general features as reported elsewhere (Deiters and Pegg, 1989; Yelash and Kraska, 1998), and discussed in Chapter 4. A ‘shield’ region is formed by three branches of the double critical end point (DCEP) curve. The diagonal lines are boundary states of critical azeotropy ($x_1^C \rightarrow 0,1$). A locus of azeotropic critical end points (ACEP) separate Types IIIA and IIIB behaviour. Tricritical point (TCP) lines separate Types I/V, VI/VII and II/IV behaviour (see Figure 5.2 for greater detail). Critical pressure step point (CPSP) (---) curves, degenerated critical pressure maximum/minimum (dCPM) (— — —) curves, van Laar points (\times), double critical end cusp points (DCECP) (?) and critical pressure landing points (CPLP) (?) are also illustrated.

Figure 5.2 is an enlargement of the global phase diagram identified by the square in Figure 5.1. In this region, we were able to identify Type IV, VI, VII and Vm behaviour.

The boundary states between these types of behaviour involve a TCP, a critical pressure set point (CPSP), a critical pressure landing point (CPLP) and a degenerate critical pressure maximum or minimum (dCPM) curve. The transition between different phase behaviour types via some of these states is illustrated in Figure 5.3. This is the first time that type VI and VII have been reported for the Guggenheim equation. The triangles mark the coordinates for calculations illustrated in Figures 5.4 to 5.7.

Interpreting the α parameter as reflecting the strength of intermolecular interaction between unlike molecules, we observe that weak unlike interaction ($\alpha < 1$) results in only variations of Types II and III behaviour. When $\alpha = 1$, Types I, II or III behaviour can be observed depending on the ratio of critical temperatures of the two components. Relatively strong unlike interaction ($\alpha > 1$) results in diversity of phenomena (Type I to VII). Types IV, VI and VII behaviour (Figure 5.2) is confined to a narrow region of moderately strong unlike interaction ($1.05 < \alpha < 1.15$) and large differences in the critical temperatures. This later observation is consistent with experiment. For example, Type VI behaviour is observed in aqueous mixtures containing a salt (Weingärtner and Steinle, 1992) for which there is a large difference in the critical temperatures of the components.

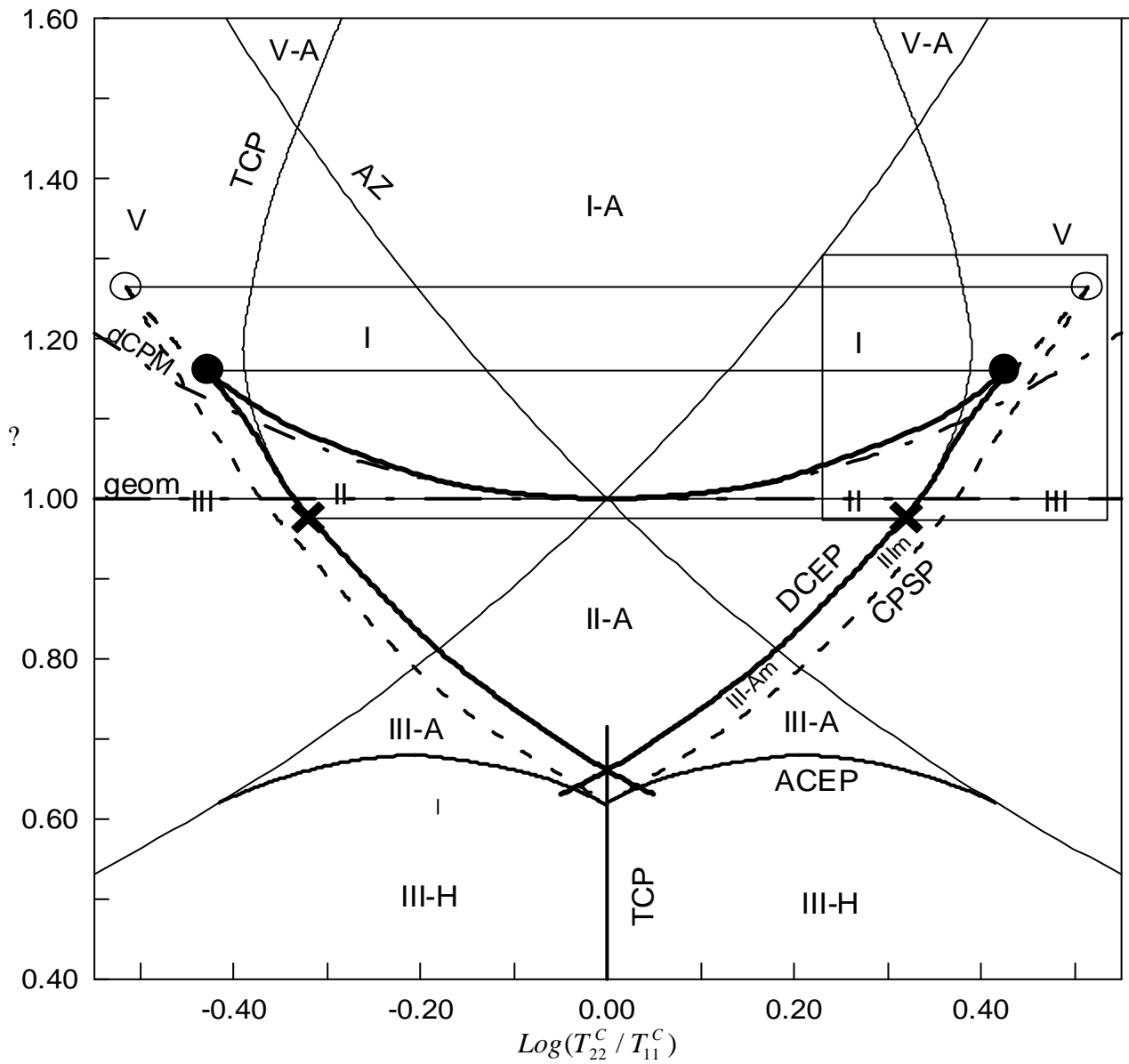


Figure 5.1 The global phase diagrams of the binary Guggenheim fluid for equal sized molecules.

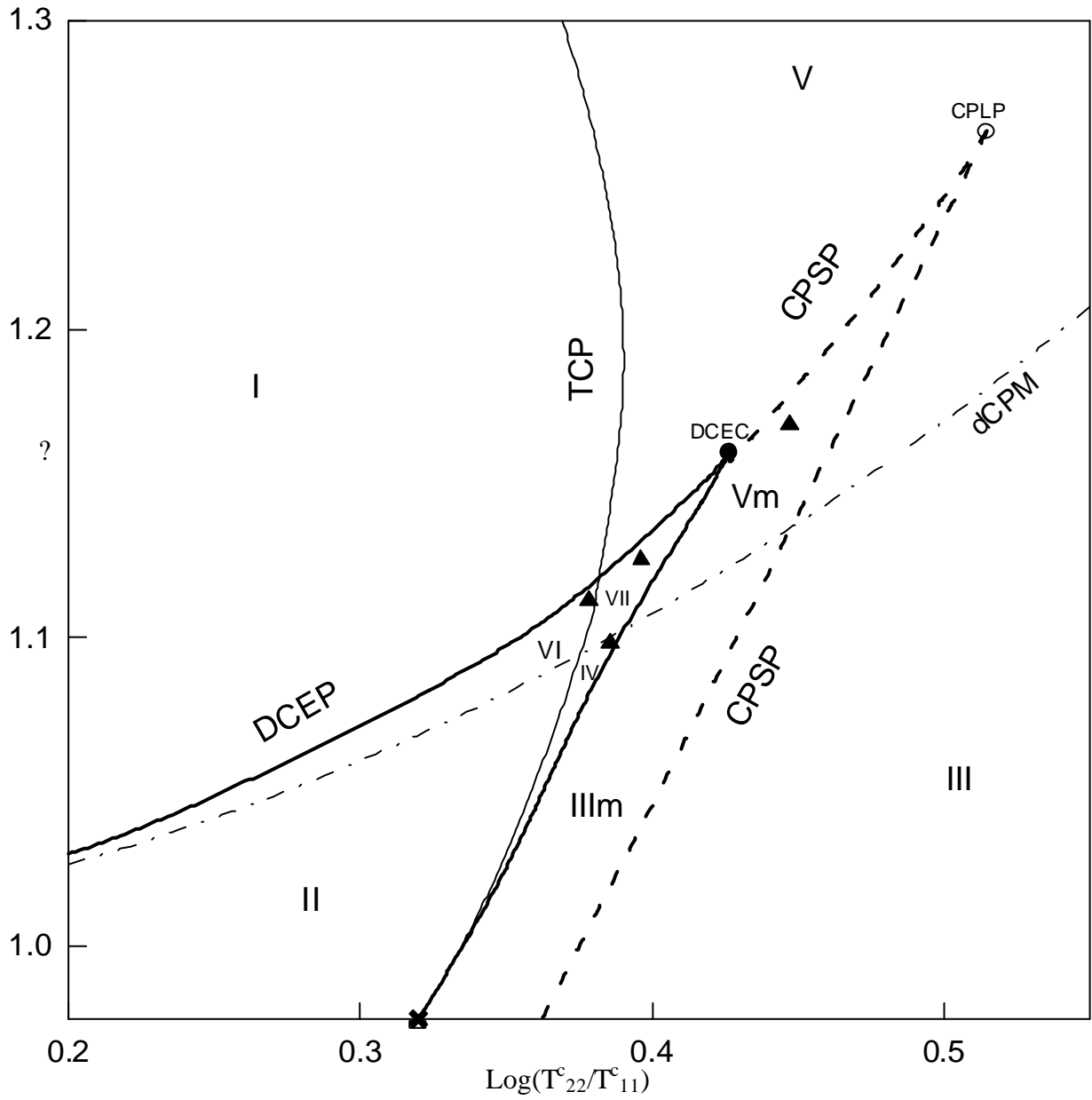


Figure 5.2 Enlargement of the global phase diagram identified by the square in Figure 5.1. The triangles mark the coordinates for calculations illustrated in Figures 5.4 – 5.7.

5.2 Possible pathways between different types of phase behaviour

We have adopted van Konynenburg and Scott's nomenclature (1980) to distinguish different subtle aspects of Type I, II, III and V behaviour. Type I-A refers to Type I behaviour with a negative azeotrope whereas Type II-A refers to Type II behaviour with a positive azeotrope. Type III-H denotes a heteroazeotrope in Type III behaviour. Phenomena denoted by III_m and III-_A_m have minimum and maximum pressures in the critical locus. Type V-A behaviour involves a negative azeotrope. It is apparent from Figure 5.1 that the global phase diagram is dominated by a triangular 'shield' formed by three branches of the double critical end point (DCEP) line which illustrates the important role of DCEP as a transition between different phase types. Similarly, the tricritical point (TCP) line is the boundary state between Type I and V behaviour.

The global phase diagram (Figure 5.1) identifies the occurrence of the various phase behaviour types and the boundaries between different states. As discussed in Chapter 4, this transition between different states commonly occurs via a TCP, a DCEP or an azeotropic critical end point (ACEP) or van Laar point. The thermodynamic criteria for these phenomena are discussed by Yelash and Kraska (1998). A considerable diversity of phase behaviour is confined to a relatively small region of the global phase diagram which is illustrated in greater detail in Figure 5.2. Figure 5.2 identifies regions in which behaviour of Type IV, V_m, VI and VII occur. As discussed in Chapter 4, the boundary states between these types of behaviour involve a TCP, a critical pressure set point (CPSP), a critical pressure landing point (CPLP) and a degenerate critical pressure maximum or minimum (dCPM). The transition between different phase behaviour types via some of these states is illustrated in Figure 5.3.

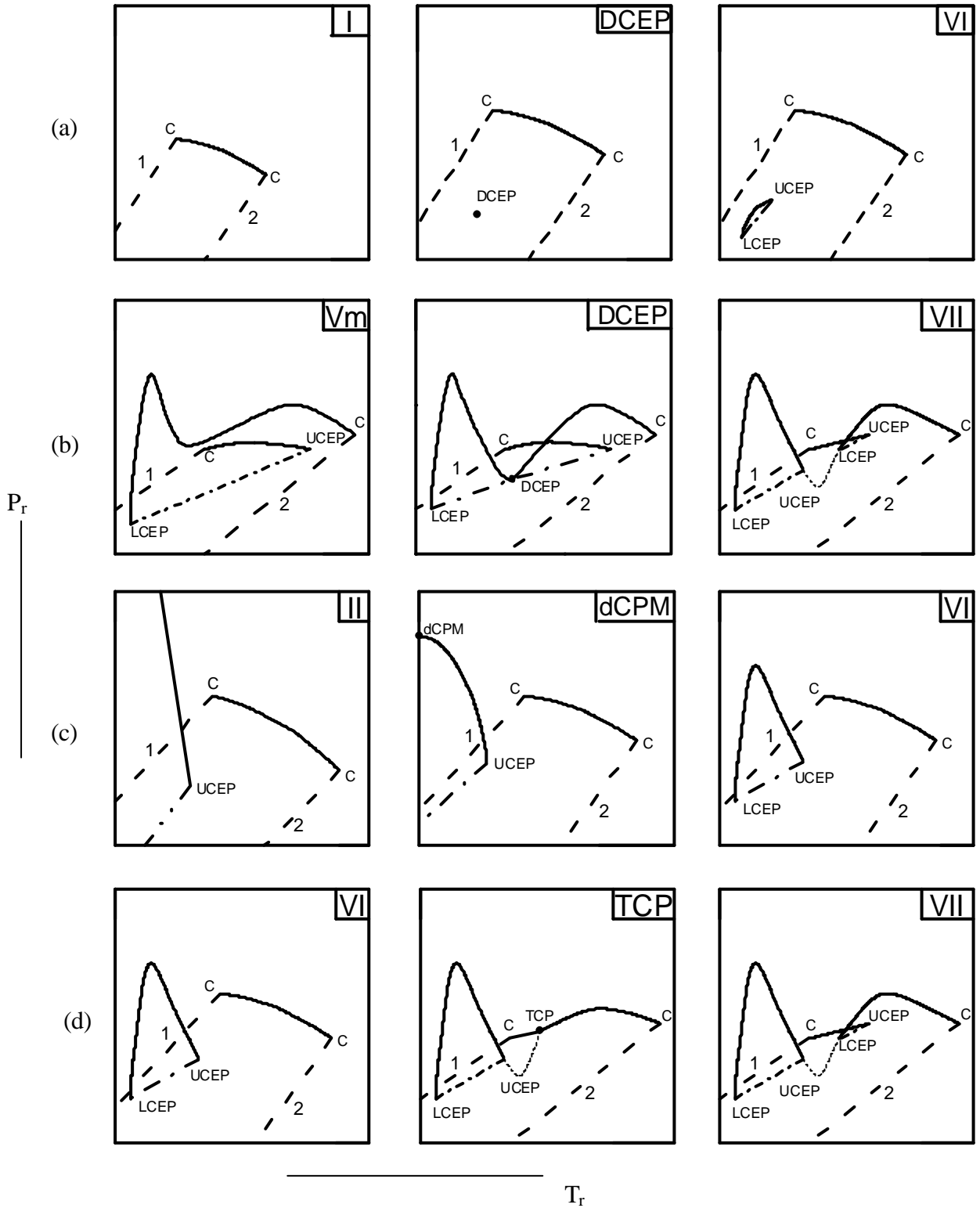


Figure 5.3. Possible pathways between different types of phase behaviour via (a) and (b) DCEP, (c) dCPM and (d) TCP.

5.3 The Calculated Critical Properties of Type IV, Vm, VI and VII

A feature of these calculations is that we have been able to predict the main features of Type IV, Vm, VI and VII phenomena using the Guggenheim equation of state. Examples of these calculations are illustrated in Figures 5.4 to 5.7.

The pressures and temperatures are reported relative to the critical properties of component one. It should be noted that there is no experimental data to indicate the existence of Type Vm or VII behaviour. Therefore in the absence of confirmation by experiment, these types of behaviour should be regarded as hypothetical only. However, the existence of Type VI behaviour is well documented experimentally (Van Pelt et al., 1991). Our calculations confirm that type VI phenomena can be predicted from hard-sphere + van der Waals interactions without requiring an additional hypothesis such as hydrogen bonding or temperature-dependent attractions. Type VI behaviour is characterized by a region of closed-loop liquid-liquid equilibria. In view of the fact that the van der Waals equation does not predict this phenomenon under any conditions, the success of both the CSvdW and Guggenheim equations suggests that repulsion plays an important role.

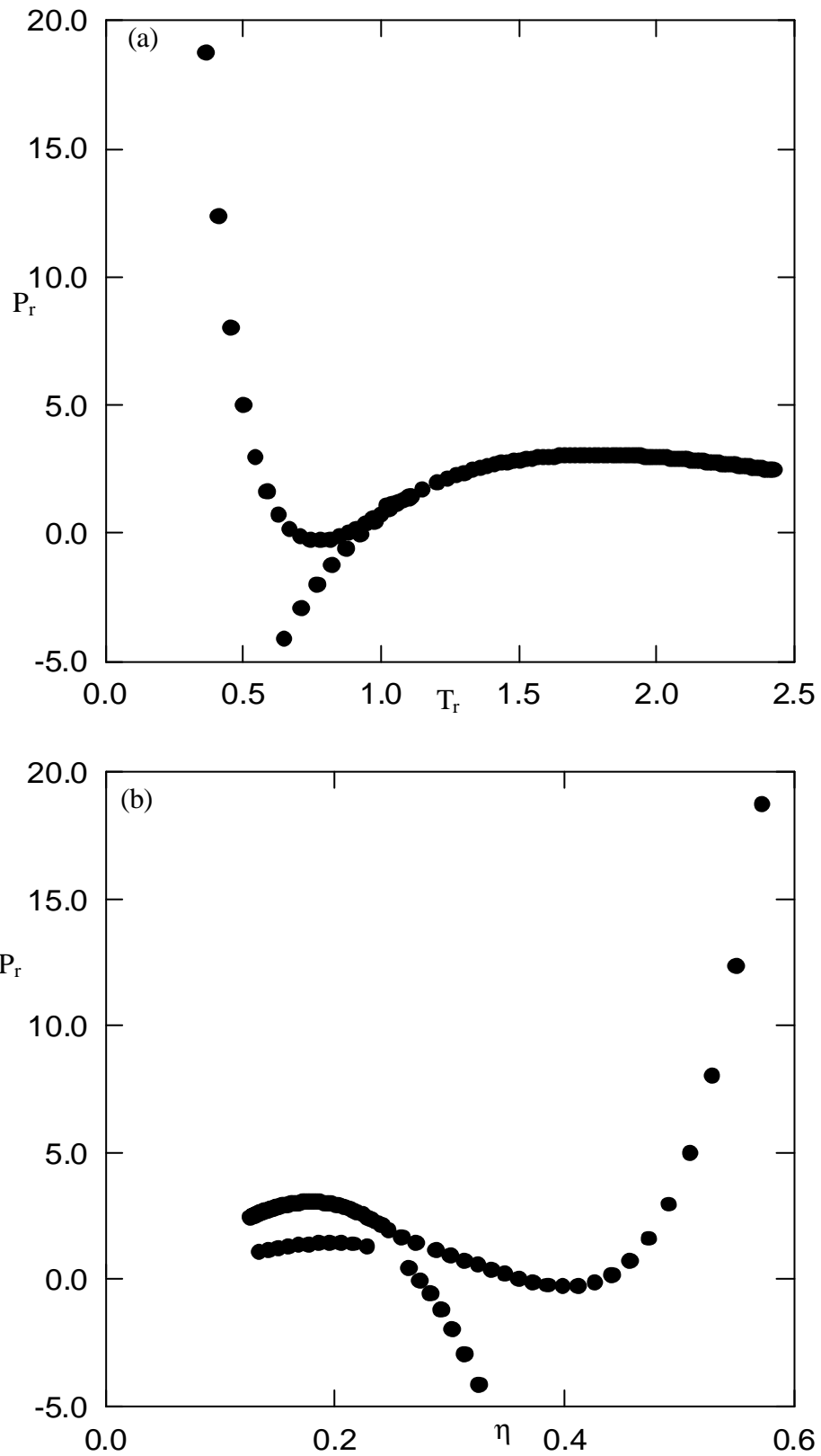


Figure 5.4. The calculated critical properties of a Type IV mixture in the (a) pressure-temperature and (b) pressure-packing fraction projections. The location of this mixture is marked in Figure 5.2 by a filled triangle at $\xi = 1.099$ and $T_{22}^c/T_{11}^c = 2.43$.

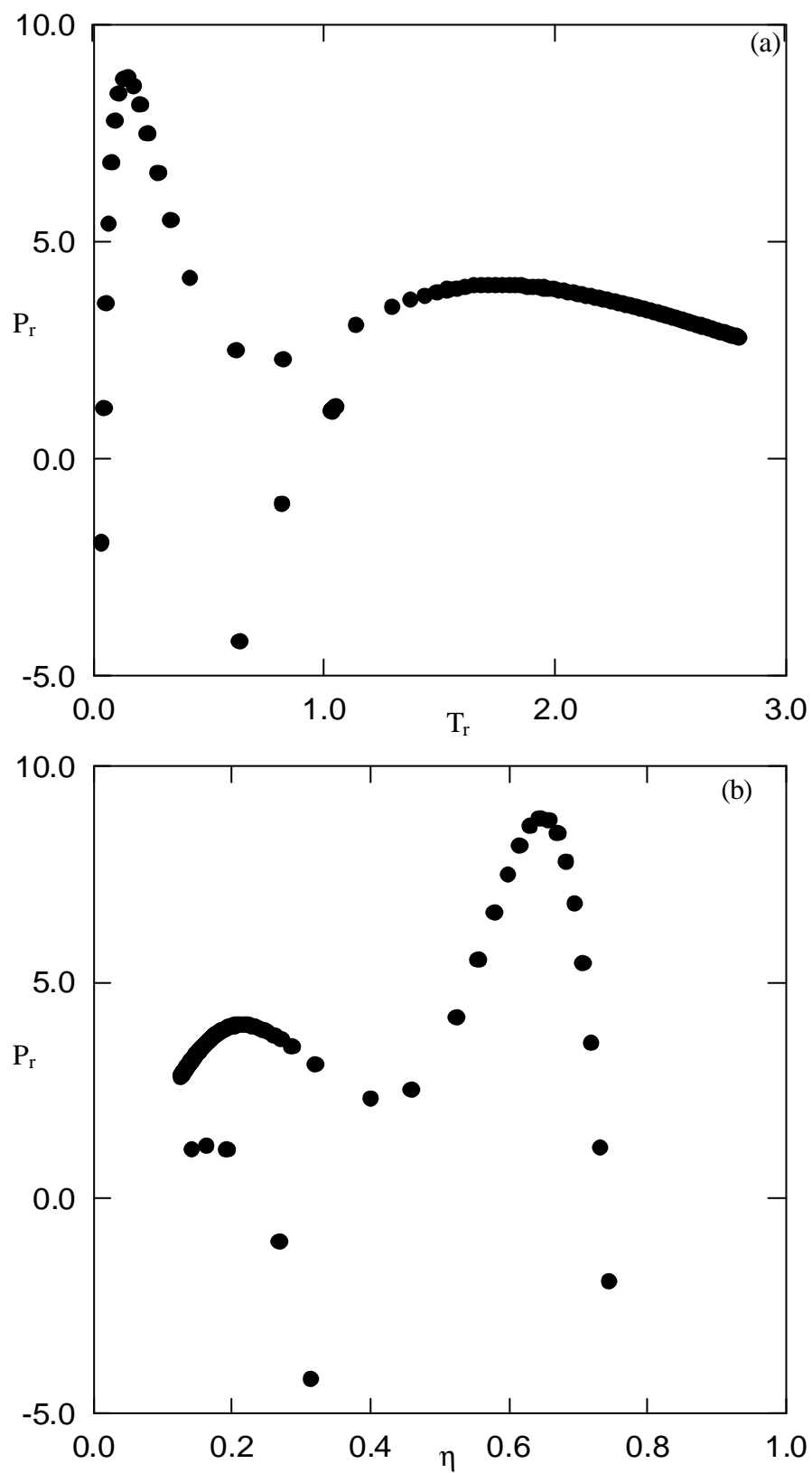


Figure 5.5. The calculated critical properties of a Type Vm mixture in the (a) pressure-temperature and (b) pressure-packing fraction projections. The location of this mixture is identified in Figure 5.2 by a filled triangle at $\xi = 1.17$ and $T_{22}^c/T_{11}^c = 2.8$.

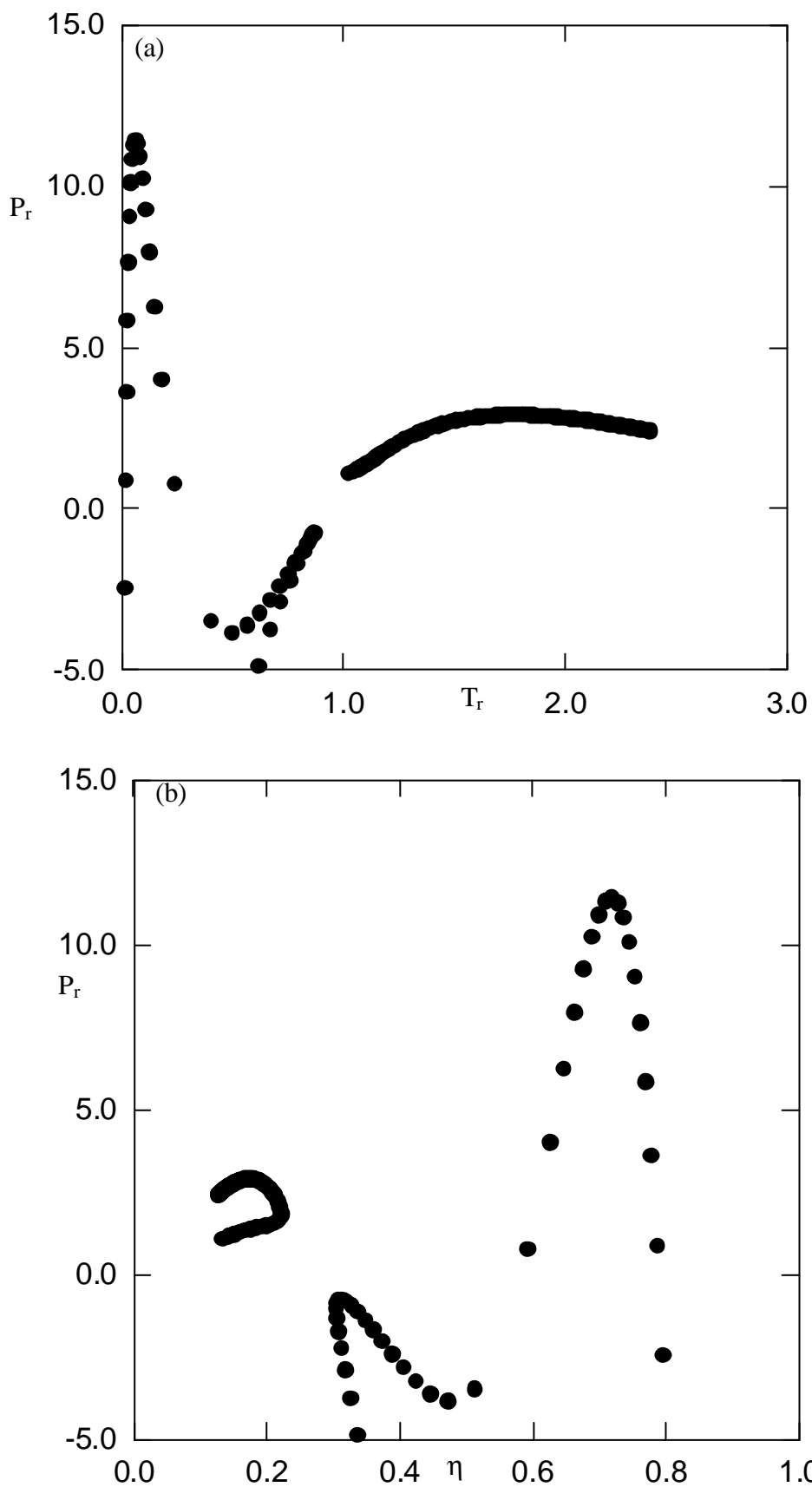


Figure 5.6. The calculated critical properties of a Type VI mixture in the (a) pressure-temperature and (b) pressure-packing fraction projections. The location of this mixture is marked in Figure 5.2 by a filled triangle at $\xi = 1.113$ and $T_{22}^c/T_{11}^c = 2.39$.

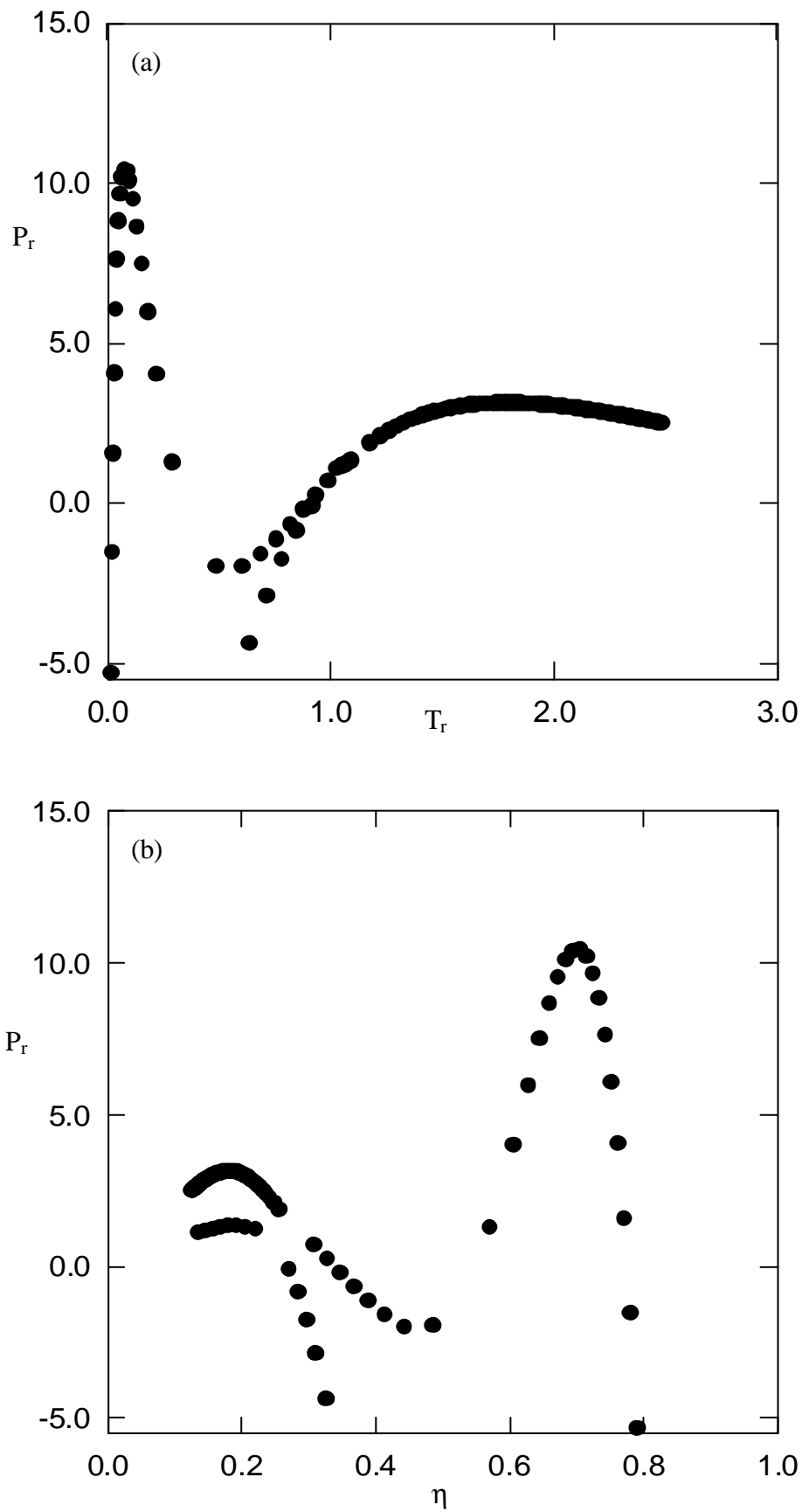


Figure 5.7. The calculated critical properties of a Type VII mixture in the (a) pressure-temperature and (b) pressure-packing fraction projections. The location of this mixture is marked in Figure 5.2 by a filled triangle at $\xi = 1.126$ and $T_{22}^c/T_{11}^c = 2.49$.

5.4 Comparison with Experiment

The global phase diagram (Figure 5.1) is based exclusively on theoretical considerations. It is of interest to determine whether real mixtures can be at least qualitatively located in the appropriate region of the diagram.

Experimented values of β for many mixtures have been calculated and reported in the literature (Sadus, 1987; Wei, 1998) for the Guggenheim equation of state. Some of those values are summarised in Tables 5.1 to 5.4. These mixture data are experimental values, because they have been determined by fitting the calculated critical properties to experimental data. These mixtures are located in the Figure 5.8.

Christou et al. (1986), Sadus and Young (1985), Mainwaring et al. (1987), Wei and Sadus (1994, 1996) and Wei et al. (1996) gave an extensive discussion on the calculation the phase behaviour of binary mixtures, the values of adjustable parameters β and γ were found more exactly comparing to experiment for some mixtures with Guggenheim equation of state, such as mixtures of ammonia + alkane or simple gases, water + 5 noble gases, carbon dioxide + hydrocarbon and tetrafluoromethane or trifluoromethane + alkane. In this work, we specifically pay attention to the magnitude of the adjustable parameter β .

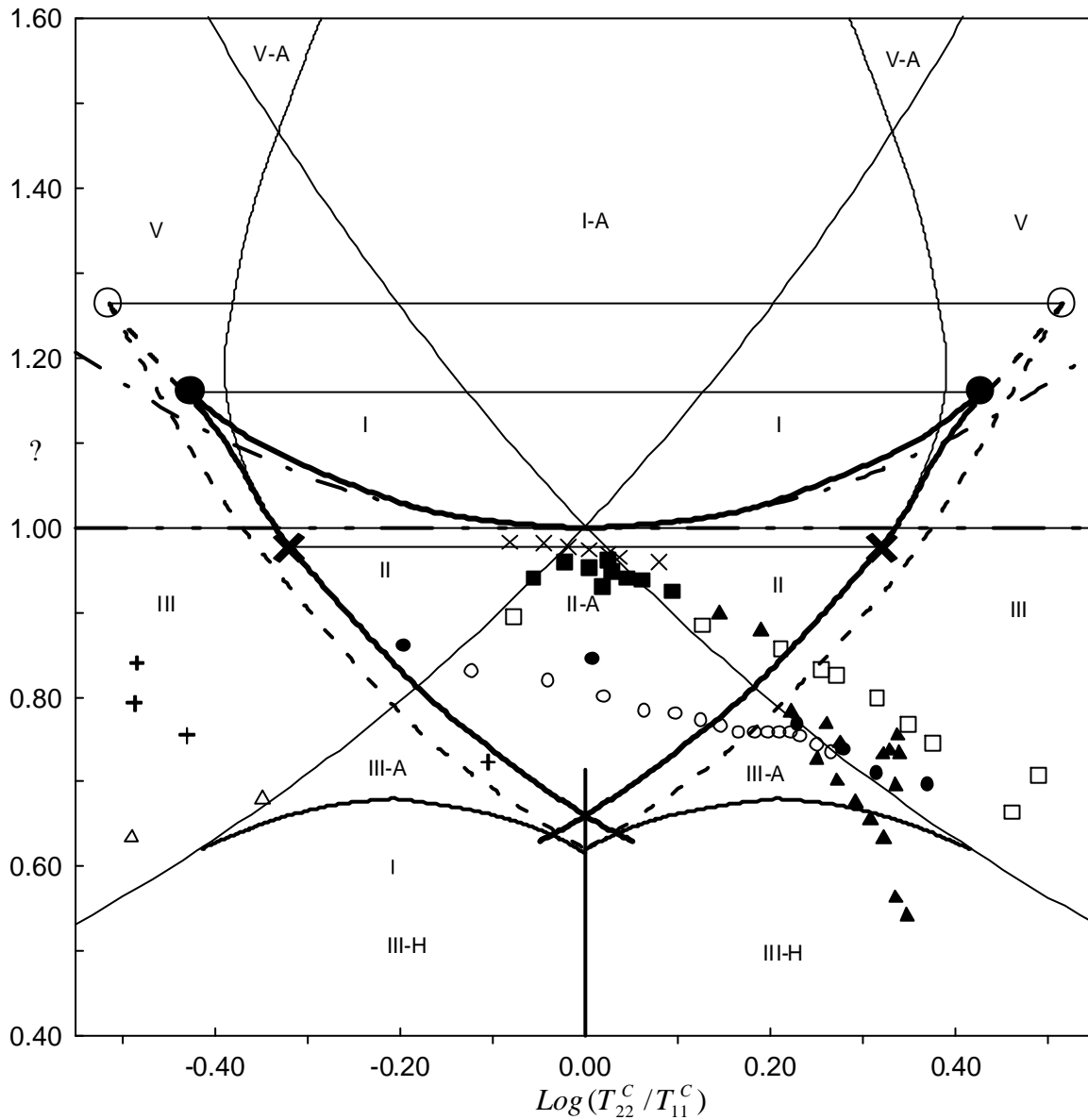


Figure 5.8 Global phase diagram showing the location of experimentally determined binary mixture data. Binary mixtures of ammonia + n-alkanes are marked by (?); Mixtures of ammonia + some simple gases are marked by (+); mixtures of water + 5 noble gases are marked by (Δ); mixtures of carbon dioxide + hydrocarbons are marked by (?); mixtures of tetrafluoromethane + alkanes are marked by (?); mixtures of trifluoromethane + alkanes are marked by (?); mixtures of benzene + n-alkanes and perfluorobenzene + alkanes are marked by (x) and (l) respectively.

Table 5.1 Values of the strength of unlike interaction χ and the logarithm of the ratio of the critical temperatures for ammonia + n-alkanes or some simple gases, water + 5 noble gases. The values of χ are obtained by Wei and Sadus (1994).

Ammonia +	Symbol	χ	$\text{Log}(T_{22}^C/T_{11}^C)$	Type	Is Located?	Ref. for Type
Ethane	?	0.83	-0.123	II	Yes	Brunner (1998)
Propane		0.819	-0.04	II	Yes	
Butane		0.8	0.021	II	Yes	
Pentane		0.783	0.064	II	Yes	
Hexane		0.78	0.097	II	Yes	
Heptane		0.772	0.125	II	Yes	
Octane		0.765	0.147	II	No	
Nonane		0.758	0.166	II	No	
Decane		0.758	0.183	II	No	
Undecane		0.758	0.197	II	No	
Dodecane		0.758	0.21	II	No	
Tridecane		0.758	0.222	II	No	
Tetradecane		0.753	0.233	II	No	
Hexadecane		0.744	0.251	II	No	
Octadecane		0.734	0.266	II	No	
Hydrogen*	+	1.1	-1.087	III	Yes	
Helium*		1.79	-1.893	III	Yes	
Nitrogen		0.793	-0.487	III	Yes	
Argon		0.755	-0.43	III	Yes	
Carbon monoxide		0.84	-0.484	III	Yes	
Sulphur hexafluoride		0.723	-0.105	III	Yes	
Water +	?					Mather et al. (1993)
Helium*		1.0	-2.096	III	Yes	
Neon*		0.56	-1.164	III	Yes	
Argon*		0.663	-0.633	III	Yes	
Krypton		0.635	-0.49	III	Yes	
Xenon		0.68	-0.349	III	Yes	

Table 5.2 Values of the strength of unlike interaction δ and the logarithm of the ratio of the critical temperatures for carbon dioxide+ hydrocarbon mixtures.

Hydrocarbon	Symbol	δ	$\text{Log}(T_{22}^C/T_{11}^C)$	Type	Is located?	Ref. for δ value and Type
Butane	δ	0.90	0.145	II	Yes	Sadus and Young (1985)
Pentane		0.88	0.189	II	Yes	
Cyclohexane		0.77	0.26	II	No	
Hexane		0.785	0.222	II	No	
n-butylbenzene		0.757	0.337	II	No	
Methylcyclohexane		0.748	0.275	II	No	
1,2,4-Trimethylbenzene		0.739	0.329	II	No	
1,2,3-Trimethylbenzene		0.735	0.339	II	No	
1,3,5-Trimethylbenzene		0.734	0.321	II	No	
Heptane		0.729	0.25	II	No	
1,4-Diethylbenzene		0.698	0.335	II	No	
Octane		0.703	0.272	II	No	
Decane		0.657	0.308	II	No	
Nonane		0.677	0.291	II	No	
Undecane		0.635	0.322	II	No	
Dodecane		0.565	0.335	II	No	
Tridecane		0.544	0.347	IV	No	

Table 5.3 Values of the strength of unlike interaction δ and the logarithm of the ratio of the critical temperatures for tetrafluoromethane or trifluoromethane + alkane mixture.

Tetrafluoromethane +	Symbol	δ	$\text{Log}(T_{22}^C / T_{11}^C)$	Type	Is located?	Ref. for δ value and Type
Methane	δ	0.893	-0.077	II	Yes	Christou et al. (1986)
Ethane		0.883	0.127	II	Yes	
Propane		0.855	0.211	II	Yes	
2-Methylpropane		0.831	0.254	III	Yes	
Butane		0.825	0.271	III	Yes	
Pentane		0.797	0.315	III	Yes	
Hexane		0.766	0.348	III	Yes	
Heptane		0.744	0.375	III	Yes	
Dodecane		0.663	0.461	III	Yes	
Cis-Decalin		0.707	0.489	III	Yes	
<hr/>						
Trifluoromethane +	δ					
Methane		0.86	-0.196	II	Yes	
Ethane		0.845	0.008	II	Yes	
Hexane		0.768	0.229	III	Yes	
Octane		0.738	0.279	III	Yes	
Decane		0.71	0.315	III	Yes	
Cis-Decalin		0.697	0.37	III	Yes	

Table 5.4 Values of the strength of unlike interaction χ and the logarithm of the ratio of the critical temperatures for benzene or perfluorobenzene + alkane mixtures.

Benzene +	Symbol	χ	$\text{Log}(T_{22}^C/T_{11}^C)$	Type	Is located?	Ref. for χ value and Type
Pentane	×	0.981	-0.081	II	Yes	Mainwaring et al. (1987)
Hexane		0.98	-0.045	II	Yes	
Heptane		0.975	-0.018	II	Yes	
Octane		0.972	0.004	II	Yes	
Nonane		0.968	0.025	II	Yes	
Decane		0.963	0.037	II	Yes	
Tridecane		0.957	0.079	II	Yes	
<hr/>						
Perfluorobenzene +	†					
Pentane		0.94	-0.056	II	Yes	
Hexane		0.959	-0.022	II	Yes	
Heptane		0.952	0.004	II	Yes	
Octane		0.948	0.029	II	Yes	
Nonane		0.94	0.045	II	Yes	
Decane		0.938	0.061	II	Yes	
Dodecane		0.925	0.094	II	Yes	
Benzene		0.962	0.025	II	Yes	
Cyclohexane		0.931	0.018	II	Yes	

In the Tables 5.1 to 5.4, the “Yes” means that the mixtures of experimental type are correctly in the Figure 5.8, and the “No” means they are not correctly located. The symbol (*) which following the name of substance means values of χ or Tr of the mixture are out the range of Figure 5.8.

It is apparent from data in Tables 5.1 to 5.4 and Figure 5.8 that the overwhelming majority of mixtures are located in the correct general region of the global phase diagram. The main exceptions are mixtures of ammonia + octane to octadecane and carbon dioxide + cyclohexane to tridecane. These mixtures occur in the Type III region instead of Type II. In these cases, the large difference in molecular size has an influence which is not accounted for by the global phase diagram.

It should be noted that the global phase diagram was developed for mixtures of equal size components and there are relatively few real systems that satisfy this requirement. However it is well known that the effect of interaction strength (ϵ) has the greatest effect on phase equilibria. The effect of size is largely restricted to shifting the boundary lines up or down. It does not change the nature of the boundary lines. Therefore, if the value of ϵ is known, we could reasonably expect real mixtures to be located on the phase diagram.

In the view of these considerations, the global phase diagram (Figure 5.1) is a reasonably good predictor of experimental phase behaviour. This is particularly the case of mixtures of Types I to III behaviour involving mixtures with only a moderate size difference between the component molecules.

References

- Boshkov, L. Z. and Yelash, L. V. (1998). Closed-Loops of Liquid-Liquid Immiscibility in Binary Mixtures Predicted from the Redlich-Kwong Equation of State, *Fluid Phase Equilib.*, **141**, 105-112.
- Brunner, E. (1988). Fluid Mixtures at High Pressures VII. Phase Separations and Critical Phenomena in 12 Binary Mixtures Containing Ammonia, *J. Chem. Thermodyn.*, **20**, 1379-1409.
- Brunner, E. (1990). Fluid Mixtures at High Pressures: IX. Phase Separation and Critical Phenomena in 23 (n-Alkane + Water) Mixtures, *J. Chem. Thermodynamics*, **22**, 335-353.
- Carnahan, N. F. and Starling, K. E. (1969). Equation of State for Nonattracting Rigid Spheres, *J. Chem. Phys.*, **51**, 635-636.
- Deiters, U. K. and Pegg, I. L. (1989). Systematic Investigation of the Phase Behaviour in Binary Fluid Mixtures. I. Calculations Based on the Redlich-Kwong Equation of State, *J. Chem. Phys.*, **90**, 6632-6641.
- Franck, E. U., Lentz, H. and Welsch, H. (1974). The System Water-Xenon at High Pressures and Temperatures, *Z. Phys. Chem.*, **93**, 95-108.
- Guggenheim, E. A. (1965). Variations on Van der Waals' Equation of State for High Densities, *Mol. Phys.*, **9**, 199-200.
- Hicks, C. P. and Young C. L. (1975). The Gas-Liquid Critical Properties of Binary Mixtures, *Chem. Rev.*, **75**, 119-175.
- Hicks, C. P., Hurle, R. L. and Young, C. L. (1977). Theoretical Prediction of Phase Behaviour at High Temperatures and Pressures for Non-Polar Mixtures: IV. Comparison with Experimental Results for Carbon Dioxide + n-Alkane Mixtures, *J. Chem. Soc. Faraday II*, **73**, 1884-1888.

- Mainwaring, D. E., Sadus, R. J. and Young, C. L. (1987). Deiters' Equation of State and Critical Phenomena, *Chem. Engng. Sci.*, **42**, 459-466.
- Mather, A. E., Sadus, R. J. and Franck, E. U. (1993). Phase Equilibria in (Water + Krypton) at Pressures from 31 MPa to 273 MPa and Temperatures from 610K to 660K and in (Water + Neon) from 45 MPa to 255 MPa and from 660K to 700K, *J. Chem. Thermodyn.*, **25**, 771-779.
- Nezbeda, I., Kolafa, J. and Smith, W. R. (1997). Global Phase Diagrams of Binary Mixtures-Systematic Basis for Describing Types of Phase Equilibrium Phenomena, *J. Chem. Soc. Faraday Trans.*, **93**, 3073-3080.
- Sadus, R. J. and Young, C. L. (1985). Phase Behaviour of Carbon Dioxide and Hydrocarbon Mixing, *Aust. J. Chem.*, **38**, 1739-1743.
- Sadus, R. J. (1987). Phase behaviour of binary and tertiary mixtures, PhD Thesis, University of Melbourne.
- Sadus, R. J. (1992). High Pressure Phase Behaviour of Multicomponent Fluid Mixtures, Elsevier, Amsterdam.
- Sadus, R. J., (1999a). Molecular Simulation of Fluids: Theory, Algorithms and Object-Oriented, Elsevier, Amsterdam.
- Sadus, R. J. (1999b). An Equation of State for Hard Convex Body Chains, *Mol. Phys.*, **97**, 1279-1284.
- Sandler, S. I. (Ed.) (1994). Models for Thermodynamic and Phase Equilibria Calculations, Marcel Dekker, New York.
- Schneider, G. M. (1978). In McGlashan, M. L. (Ed.), Chemical Thermodynamics: 2. A Specialist Periodical Report, The Chemical Society, London.
- Schneider, G. M. (1991). High Pressure Investigations on Fluid Systems. A Challenge to Experiment, Theory and Application, *J. Chem. Thermodyn.*, **23**, 301-326.

- Van Konynenburg, P. H. and Scott, R. L. (1980). Critical Lines and Phase Equilibria in Binary van der Waals Mixtures, *Philos. Trans. Roy. Soc. London A*, **298**, 495-540.
- Van Pelt, A., Peters, C. J. and de Swaan Arons, J. (1991). Liquid-Liquid Immiscibility Loops Predicted with the Simplified-Perturbed-Hard-Chain Theory, *J. Chem. Phys.*, **95**, 7569-7575.
- Wang, J. L., Wu, G. W. and Sadus, R. J. (2000). Closed-Loop Liquid-Liquid Equilibria and the Global Phase Behaviour of Binary Mixtures Involving Hard-Sphere + van der Waals Interactions, *Mol. Phys.*, **98**, 715-723.
- Wei, Y. S. and Sadus, R. J. (1994). Calculation of the Critical High Pressure Liquid-liquid Phase Equilibria of Binary Mixtures Containing Ammonia: Unlike Interaction Parameters for the Heilig-Franck Equation of State, *Fluid Phase Equilib.*, **101**, 89-99.
- Wei, Y. S. and Sadus, R. J. (1996). Vapour-liquid and Liquid-liquid Phase Equilibria of Binary Mixtures Containing Helium: Comparison of Experiment with Predictions Using Equations of State, *Fluid Phase Equilib.*, **122**, 1-15.
- Wei, Y. S., Sadus, R. J. and Franck, E. U. (1996). Binary Mixtures of Water + Five Noble Gases: Comparison of Binodal and Critical Curves at High Pressures, *Fluid Phase Equilib.*, **123**, 1-15.
- Wei, Y. S. (1998). Prediction of the Fluid Phase Equilibria of Binary and Ternary Mixtures, PhD Thesis, Swinburne University of Technology.
- Wei, Y. S. and Sadus, R. J., (1999). Phase Behaviour of Ternary Mixtures: a Theoretical Investigation of the Critical Properties of Mixtures with Equal Size Components, *Phys. Chem. Chem. Phys.*, **1**, 4329-4336.
- Wei, Y. S. and Sadus, R. J. (2000). Equations of State for the Calculation of Fluid-Phase Equilibria, *AIChE J.*, **46**, 169-196.

- Weingärtner, H. and Steinle, E. (1992). P, T, x Surface of Liquid - Liquid Immiscibility in Aqueous Solutions of Tetraalkylammonium Salts, *J. Phys. Chem.*, **96**, 2407-2409.
- Yelash, L. V. and Kraska, T. (1998). Closed-Loops of Liquid-Liquid Immiscibility in Binary Mixtures of Equal Sized Molecules Predicted with a Simple Theoretical Equation of State, *Ber. Bunsenges. Phys. Chem.*, **102**, 213-223.